Progress In Electromagnetics Research, PIER 42, 27–48, 2003

ANALYSIS OF THE REFLECTION PROPERTIES IN ELECTROMAGNETIC BANDGAP COPLANAR WAVEGUIDES LOADED WITH REACTIVE ELEMENTS

F. Martín

Departament d'Enginyeria Electrònica
Universitat Autònoma de Barcelona
08193 BELLATERRA (Barcelona), Spain

F. Falcone

Departamento de Ingeniería Eléctrica y Electrónica
Universidad Pública
de Navarra, 31006 Pamplona, Spain

J. Bonache

Departament d'Enginyeria Electrònica
Universitat Autònoma de Barcelona
08193 BELLATERRA (Barcelona), Spain

T. Lopetegi, M. A. G. Laso, and M. Sorolla

Departamento de Ingeniería Eléctrica y Electrónica
Universidad Pública
de Navarra, 31006 Pamplona, Spain

Abstract—In this work, we study the reflection properties of coplanar waveguides (CPW) periodically loaded with shunt connected capacitances and periodically perturbed by varying the slot width. These structures are of interest because the low pass frequency response with spurious frequency bands, inherent to the presence of capacitors, can be improved. This is achieved through the attenuation of frequency parasitics that is obtained by the introduction of slot width modulation. Both sinusoidal and square wave patterns are considered and the effects of the relative position of reactive elements with regard to the perturbation geometry is analysed. According to coupled

mode theory, the central frequencies of the rejected bands in periodic transmission media are given by the spectrum of the perturbation function. However, it is demonstrated that, due to the presence of capacitors, multiple spurious bands can be simultaneously suppressed even in the case of a singly tuned (sinusoidal) perturbation geometry. This result points out that the frequency selective behaviour associated to the presence of slot width modulation can not be interpreted in the framework of coupled mode theory, since the rejection of spurious bands in periodic loaded CPWs is not merely given by the spectrum of the perturbation geometry.

1. INTRODUCTION

Transmission lines periodically loaded with shunt-connected reactances are of interest for the fabrication of microwave and millimeter wave filters, phase shifters and frequency multipliers. Due to periodicity, these structures exhibit significant dispersion as well as passband-stopbands in the frequency response, on which its filtering properties rely. If the shunt reactances are voltage controlled capacitors the device can behave as a time delay phase shifter [1] or as a frequency multiplier [2]. In the first case propagation velocity is tailored by means of an external bias applied to the loading capacitors. (Micro-Electro-Mechanical capacitive Switches -MEMS- have been recently proposed for the fabrication of delay lines due to their low-loss performance and high capacitance ratio achievable [3, 4]). As frequency multipliers, the devices require large feeding signals, resulting in nonlinear operation and hence harmonic generation [5]. The key advantage of these distributed structures over conventional designs is the wide operating bandwidth, which can be extended up to several tens of GHz, or even more, depending on the available technology.

From the fabrication point of view, device grounding is necessary in any of the cited applications. Therefore coplanar waveguide (CPW) transmission lines are appropriate, since no electrical connections are required across the substrate provided signal strip and ground planes are at the same level. In addition, CPWs are less dispersive than other transmission lines such as microstrip and radiation losses are generally of less significance [6].

Regardless of the application and specific transmission line medium, a key parameter for the design of periodic loaded transmission lines is the Bragg frequency. This delimits the first frequency band and hence the cutoff frequency of the device operating as low pass filter. Also, it determines the operating bandwidth in time delay phase shifters and frequency multipliers. The device frequency response is thus related to the Bragg frequency, which is dependent on the value and distance between adjacent reactances as well as on the geometry and physical parameters of the line. However, the frequency selective behaviour of these structures can be enhanced by using the electromagnetic bandgap (EBG) concept [7]. This can add flexibility to the designs, which can be of interest for the optimisation of structures based on transmission lines periodic loaded with shunt reactances. For instance, low pass filters can be improved by rejecting the spurious passbands that inevitably appear above the Bragg frequency. In distributed frequency multipliers, EBGs can potentially be used as a way to improve conversion efficiency to the desired harmonic. Finally, in delay lines, the electrical characteristics of the line can be tailored by the use of EBGs with the benefit of a major design flexibility.

EBGs are periodic structures which exhibit transmission behaviour analogous to carrier transport in semiconductors. Initially applied to the optical domain as photonic bandgaps (PBGs), due to the scalability in frequency, EBGs have been also applied to the optimisation of microwave and millimetre wave devices fabricated in planar circuit technology [8]. Planar EBGs are essentially transmission lines with periodic perturbations in wave impedance. This produces Bragg reflection in some frequency bands, roughly given by the spectrum of the coupling coefficient [9, 10], which is closely related to the wave impedance of the line and hence line geometry. The modulation of the wave impedance can be achieved by drilling holes in the substrate [11], by etching periodic patterns in the ground plane [12–15], or by varying the geometry of the signal strip [16] (or a combination of them). So far, most of the applications of EBG structures have been carried out in microstrip technology. To cite some examples, the method has been successfully applied to the elimination of spurious bands in distributed bandpass filters [16], to enhance efficiency in broad-band

power amplifiers by harmonic tuning [17], or to reduce phase noise in microwave oscillators [18]. In coplanar waveguide technology, uniplanar EBG structures have been recently proposed for the fabrication of filters and resonators based on the perturbation of line geometry [19], and EBG effects have been experimentally demonstrated where perturbation is implemented by etching patterns in the ground plane following a periodic structure [20]. Also, a miniaturized low pass filter has been recently proposed based on the slow wave effect and stop band characteristics of a CPW structure with capacitive and inductive coupling at periodic positions [21].

The present work is devoted to the application of EBG structures to CPWs periodically loaded with reactive elements (from now on these structures will be referred to as PL-EBG-CPW). The investigation of these structures is of interest since two types of periodicity are simultaneously present in the line: that derived from the shunt reactances, and that caused by the modulation of the wave impedance. To be more specific, we will concentrate on CPWs periodically loaded with constant capacitances and periodically perturbed by varying the distance between the central strip and ground planes. The main aim is to suppress the undesired passbands above the Bragg frequency to improve the performance of the structure as low pass filter. As will be shown later, the combination of geometry modulation and shunt capacitances, enhances the reflection properties of the structure, being possible the rejection of multiple frequency bands by means of very simple perturbation geometry. This is the relevant result of this work and points out that coupled mode theory can not be directly applied to the design of PL-EBG-CPW structures, due to the lack of correspondence between the rejected bands and the Fourier components of the EBG geometry.

The work is organised as follows: in Section 2, the frequency selective behaviour of PL-EBG-CPW structures is studied within the framework of microwave network theory. Since the unperturbed structure (PL-CPW) is already dispersive (due to the presence of capacitances), frequency tuning (i.e., rejection of spurious bands) requires the knowledge of the dispersion relation for the PL-CPW. From this, we determine the perturbation periods which are necessary to tune the device at the desired bands. An estimation of the rejected bands in the resulting PL-EBG-CPWs is done by numerical calculation of the dispersion relation. Different perturbation geometries (sinusoidal and square) are considered and the effects of the relative phase between the EBG structure and capacitor's periodicity is analysed. In Section 3 a planar equivalent circuit of the PL-EBG-CPW structure is proposed and used to understand the excess of rejected

bands inferred from the analysis of the previous section. Section 4 is focused on the validation of the analytical results. Both circuit simulation and experimental results, obtained on fabricated structures, are found to be in agreement with the theory. Finally, in Section 5, the main conclusions of the work are presented.

2. MICROWAVE NETWORK ANALYSIS OF PL-EBG-CPW STRUCTURE

For a given perturbation geometry, three parameters are required to specify a EBG: the period (λ_T) and amplitude of the perturbation, and the number of cascading stages. The latter two allow rejection level control, while the former determines the center frequency of the rejected band, according to the Bragg condition, i.e., $f_o = v_{pL}/2\lambda_T$ (where v_{pL} is the phase velocity of the loaded unperturbed line) [8]. With regard to the magnitude of rejection, this is limited by the number of cascading stages which is in turn constrained by device dimensions, usually not allowed to exceed certain limits. Also, the perturbation amplitude is limited by the spatial resolution of the layout generation system (drilling machine or optical system). In reference to frequency tuning (Bragg condition), it has been usually assumed that the propagation velocity is the same as that of the unperturbed transmission line. However, for the suppression of spurious bands in PL-EBG-CPW structures, some caution must be taken, provided the unperturbed PL-CPW is very dispersive near and above the Bragg frequency and v_{pL} is thus frequency dependent. This means that, to determine the period of the perturbation, it is necessary to use the dispersion relation of the PL-CPW, which is given by [22]:

$$\cos\beta l = \cos kl - \frac{\omega C_{ls} Z_o}{2} \sin kl \tag{1}$$

where k and β are the phase constants of the unloaded and loaded line, respectively, C_{ls} the loading capacitances, l the distance between adjacent capacitances and Z_o the characteristic (or wave) impedance of CPW sections between adjacent capacitances. The dispersion relation is depicted in a Brillouin diagram in Figure 1, where $\theta = kl$ is proportional to frequency and $\varphi = \beta l$. This is a representation in a reduced zone, i.e., $0 \leq \varphi \leq \pi$. Actually, this interval corresponds to the first frequency band ($f < f_B$), while the following passbands are delimited by phase constants given by the intervals $n\pi \leq \varphi \leq (n+1)\pi$, where $n = 1, 2, 3 \ldots$ enumerates the spurious bands. The passbands of the structure (determined by those frequencies satisfying the condition $|\cos\beta l| < 1$) are very narrow above the Bragg frequency. Thus, the

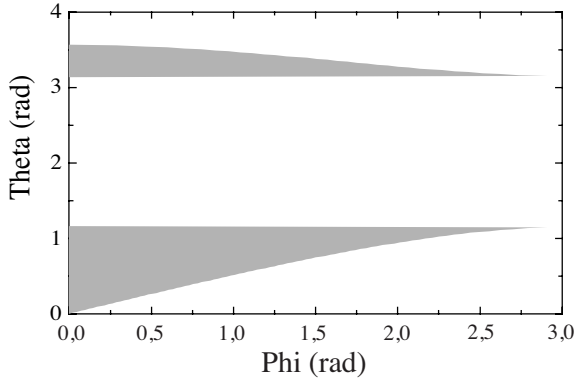

Figure 1. Dispersion diagram of an arbitrary periodic loaded unperturbed coplanar waveguide (PL-CPW) depicted in a reduced Brillouin zone.

rejection of spurious bands is expected to be efficient provided the period of the perturbation is determined from the Bragg condition ($\lambda_T = v_{pL}/2f_o = \pi/\beta$) with $\varphi = \beta l$ in the center of the interval corresponding to the spurious band to be suppressed. According to coupled mode theory, multiple bands can be suppressed if the wave impedance is perturbed by a periodic function with harmonic content. Since the wave impedance is related to line geometry, by choosing a square wave perturbation pattern, attenuation in multiple frequency bands is possible. By virtue of the previous words, if the PL-EBG-CPW is perturbed by means of a square wave function, and the period of the perturbation is chosen according to $\lambda_T = 2l$, then those bands with center φ given by $\varphi = (2n+1)\cdot\pi/2$ (with $n = 0, 1, 2, 3\ldots$) can potentially be eliminated. Following the dispersion diagram, this corresponds to all spurious bands, but also includes first band attenuation in a frequency interval close to the Bragg frequency. Alternatively, to maintain invariable the device response below the Bragg frequency, the perturbation period can be selected according to $\lambda_T = 2l/3$. The penalty in this case is the elimination of only those spurious bands satisfying $\varphi = n\cdot 3\pi/2$, with $n = 1, 3, 5\ldots$ Nevertheless, the presence of capacitors in the PL-EBG-CPW structure might give rise to interaction effects with the periodic perturbation. These effects can modify the results expected from coupled mode theory, provided this theory does not account for the presence of lumped devices. Therefore, it is necessary to make a detailed analysis of the reflection-transmission properties of PL-EBG-CPWs. To this end, the dispersion relation of the structure will be obtained. The two cases corresponding

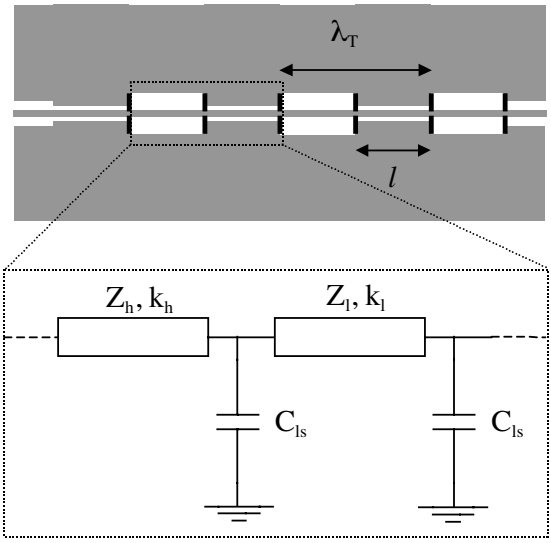

Figure 2. Layout of the PL-EBG-CPW (case A) and schematic of the basic cell. The shunt-connected capacitors are represented by black rectangles placed in the layout steps.

to the cited periods will be studied, and sinusoidal perturbation geometries will be also considered for comparison purposes.

Case A: $\lambda_T = 2l$

To obtain the dispersion relation of the structure, it is necessary to calculate the transmission (T) matrix of the elementary cell (Figure 2). This can be obtained from the product of each cascading section, including impedance steps:

$$T = \frac{1}{16 Z_l Z_h} \begin{pmatrix} e^{jk_h l} & 0 \\ 0 & e^{-jk_h l} \end{pmatrix} \begin{pmatrix} Z_h + Z_l & Z_l - Z_h \\ Z_l - Z_h & Z_h + Z_l \end{pmatrix} \begin{pmatrix} 2 + j\omega C_{ls} Z_l & j\omega C_{ls} Z_l \\ -j\omega C_{ls} Z_l & 2 - j\omega C_{ls} Z_l \end{pmatrix} \begin{pmatrix} e^{jk_l l} & 0 \\ 0 & e^{-jk_l l} \end{pmatrix} \begin{pmatrix} Z_h + Z_l & Z_h - Z_l \\ Z_h - Z_l & Z_h + Z_l \end{pmatrix} \begin{pmatrix} 2 + j\omega C_{ls} Z_h & j\omega C_{ls} Z_h \\ -j\omega C_{ls} Z_h & 2 - j\omega C_{ls} Z_h \end{pmatrix} \tag{2}$$

$Z_l(Z_h)$ are the characteristic impedances of the low(high) impedance transmission lines of the EBG structure and $k_l(k_h)$ the corresponding propagation constants. From (2), the dispersion relation can be obtained according to [22]:

$$\cos 2\beta l = \frac{T_{11} + T_{22}}{2} \tag{3}$$

and after some tedious calculation:

$$\cos 2\beta l = \frac{1}{4Z_l Z_h}\left[2\left(Z_S\cos\frac{\theta_S}{2} - \omega C_{ls} Z_l Z_h \sin\frac{\theta_S}{2}\right)^2 - 2\left(Z_D\cos\frac{\theta_D}{2} + \omega C_{ls} Z_l Z_h \sin\frac{\theta_D}{2}\right)^2 - 4Z_l Z_h\right] \quad (4)$$

where $Z_S = Z_l + Z_h$, $Z_D = Z_h - Z_l$, $\theta_S = (k_h + k_l)l$ and $\theta_D = (k_h - k_l)l$. Expression (4) reduces to (1) if $Z_l = Z_h$ ($k_l = k_h$). However, since the basic cell for the PL-EBG-CPW contains two capacitor stages the dispersion relation (4) appears formally different than (1). Inspection of (4) reveals that those frequencies satisfying $\beta l = (2n+1)\cdot\pi/2$ ($n = 0, 1, 2, 3\ldots$) are rejected due to the second term of the right hand side, which is always negative. Also, since the magnitude of this term increases with frequency, the level of rejection is expected to increase with spurious band order. Figure 3a, where the right hand side of (4) is depicted, confirms the previous statement. Due to the scale of the vertical axis, attenuation in the first band is scarcely visible, but the modulus of the first minimum exceeds the value of 1. Thus, by using step variations in wave impedance (or line geometry) and a perturbation period corresponding to two capacitor stages, the suppressed bands are those expected by coupled mode theory.

Let us now consider a continuous sinusoidal variation of wave impedance (which approximately corresponds to a sinusoid geometry). In this case it is not possible to obtain an analytical expression for the dispersion relation, but we can obtain the right hand side of (3) by numerical calculation. To this end, the elementary cell has been divided into uniform transmission line sections of variable impedance and very small length, and the overall transmission matrix has been obtained by means of an iterative algorithm. It has been found that decomposition into 50 transmission line sections provides convergence of results, while the calculation time does not exceed several seconds (in a Pentium III microprocessor). The result of the calculation is shown in Figure 3(b). Surprisingly, not only attenuation in the first band is obtained; spurious passband rejection is also achieved, in spite of the singly tuned perturbation function considered. For comparison purposes, let us now consider a PL-EBG-CPW structure with the same perturbation function (sinusoid) but with capacitors placed at those positions where the characteristic impedance reaches a maximum or minimum (Figure 3c). In this case, multiple rejection of frequency bands occurs but the attenuation level decreases dramatically. These results clearly point out that coupled mode theory can not be directly applied to control the frequency selective behaviour in PL-

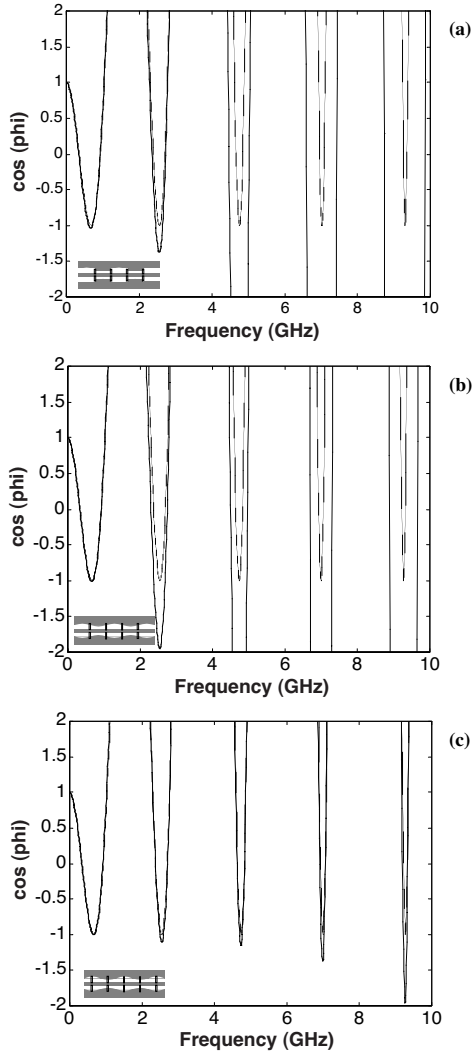

Figure 3. Representation of $\cos(\varphi)$ for the PL-EBG-CPW (bold lines) and PL-CPW (thin lines) structures considered in case A ($\lambda_T = 2l$). $\varphi = 2\beta l$ to account for the two capacitor stages of the elementary cell of the PL-EBG-CPW structure. The perturbation geometries for the PL-EBG-CPW structures are: (a) stepped, (b) sinusoid and (c) sinusoid with capacitor locations shifted $\pi/2$. Transmission occurs only for those frequencies satisfying the condition $|\cos(\varphi)| < 1$. To obtain these curves, those electrical parameters of Section 4 (case A) have been used.

EBG-CPW structures. Since the placement of capacitors relative to the perturbation geometry is relevant in determining the frequency response of the device, it is clear that interaction effects between capacitors and the EBG structure should be present and might explain the previous results. However, before this interpretation, we will focus on PL-EBG-CPWs designed to suppress the first spurious band.

Case B: $\lambda_T = 2l/3$

As has been previously indicated, the foresight of coupled mode theory for square wave perturbation with $\lambda_T = 2l/3$ is the elimination of only those spurious bands characterised by $\beta l = n \cdot 3\pi/2$ ($n = 1, 3, 5 \ldots$), leaving the first band unaltered. Let us proceed as in the previous case to obtain the frequency selective behaviour of the structure. Even though the characteristic impedance changes in steps, the elementary cell contains in this case three EBG periods (i.e. two capacitances), making the analytic calculation of the dispersion relation very cumbersome. Therefore we have obtained the transmission matrix numerically. In Figure 4a, the right hand side of (3) is depicted. The result confirms that up to the Bragg frequency no changes are produced by the EBG structure. Above this frequency, rejection in all spurious bands is visible. This result is of great interest since by the use of a very simple perturbation geometry, undesired frequency bands can potentially be eliminated. In Figures 4b and 4c, $\cos(2\beta l)$ is represented for the sinusoid EBG structure with and without relative phase variation, respectively. Once again, multiple frequency bands are rejected although attenuation is less effective if capacitors are placed in locations corresponding to extreme values of line impedance.

3. INTERPRETATION OF RESULTS AND DISCUSSION

Clearly, the presence of shunt capacitors enhances the reflection properties of PL-EBG-CPWs. The interpretation of the results of the previous section is not simple since coupled mode theory does not account for the presence of lumped elements. However, we can model the PL-EBG-CPW by means of a completely planar circuit in which the shunt capacitances are replaced by low impedance transmission line sections of length and width frequency dependent. In such a way, the presence of lumped elements is avoided and coupled mode theory is applicable. It is well known that a two-port network containing a shunt-connected capacitor is equivalent to a low impedance transmission line section [22]. The single requirement is that the electrical length of the line must be clearly below $\pi/4$ at the

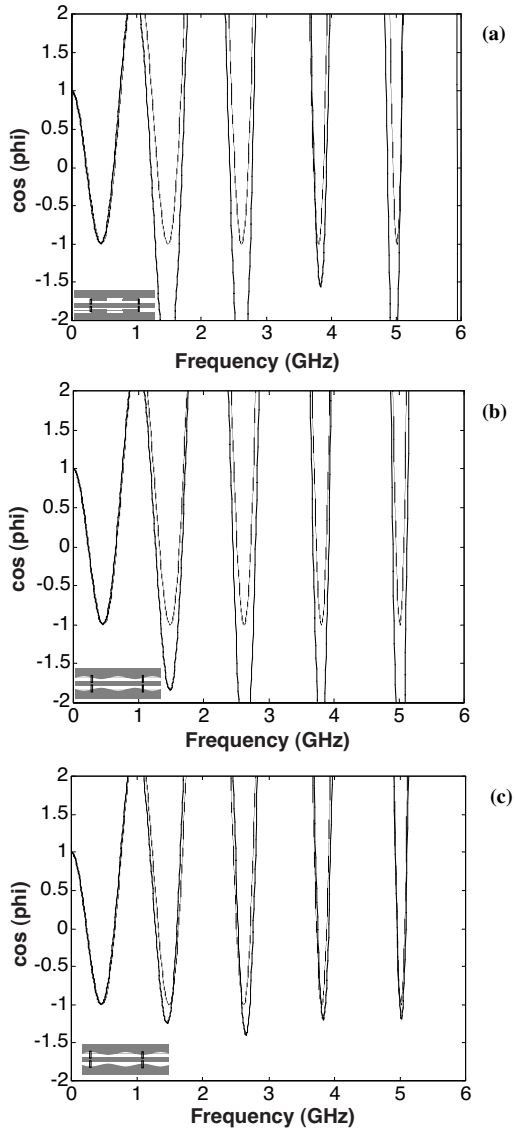

Figure 4. Representation of $\cos(\varphi)$ for the PL-EBG-CPW (bold lines) and PL-CPW (thin lines) structures considered in case B ($\lambda_T = 2l/3$). As in Fig. 3, $\varphi = 2\beta l$. The perturbation geometries for the PL-EBG-CPW structures are: (a) stepped, (b) sinusoid and (c) sinusoid with capacitor locations shifted $\pi/2$. To obtain these curves, those electrical parameters of Section 4 (case B) have been used.

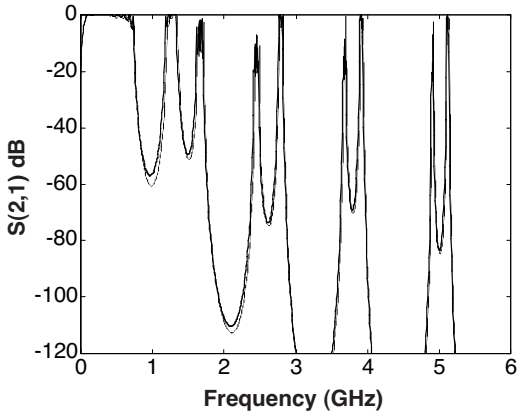

Figure 5. Comparison of the frequency response of the PL-EBG-CPW of Figure 4b (thin line) and that obtained for the planar equivalent circuit with capacitors replaced with transmission line sections (bold line). Undistinguishable results are obtained except at very low frequencies.

frequency of interest. The length (d_{eq}) and characteristic impedance (Z_{eq}) of the equivalent transmission line are related to the capacitor value by:

$$kd_{eq} = Z_{eq}\omega C_{ls} \tag{5}$$

To guaranty the previous condition, the electrical length is set to $kd_{eq} = \pi/10$. Therefore, the characteristic impedance of the equivalent transmission line section has a frequency dependence given by:

$$Z_{eq} = \frac{\pi}{10\omega C_{ls}} \tag{6}$$

To verify the validity of the model, in Figure 5 are compared the transmission coefficients of a PL-EBG-CPW perturbed by means of a sinusoidal function with $\lambda_T = 2l/3$, and the same structure with the capacitances replaced by transmission line sections. As can be seen, the results are undistinguishable except at very small frequencies, where the low impedance approximation fails. The key point to understand the results of the previous section is that the geometry of the planar equivalent circuit (with capacitors replaced by low impedance transmission line sections) is not merely given by the addition of the perturbation function and the stepped geometry related to the presence of low impedance transmission line sections. If this were the case, then the rejected frequencies would be those

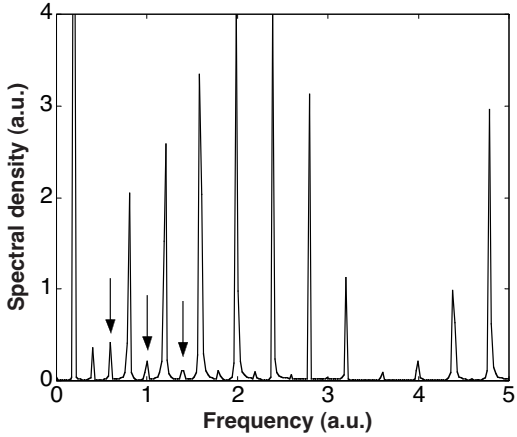

Figure 6. Fourier Transform of the coupling coefficient corresponding to the planar circuit model of a PL-EBG-CPW with sinusoidal perturbation and $\lambda_T = 2l$. Since the result is qualitative, shunt capacitors have been replaced by short and low impedance transmission line sections of constant dimensions. The arrows indicate the central frequency of the spurious rejected bands.

corresponding to the presence of capacitances, plus rejected bands centred at frequencies roughly given by the spectrum of the wave impedance (or line geometry) of the unloaded line. However, the layout of the planar equivalent circuit does not obey this additive law. The result is the presence of additional rejected bands that are consequence of new Fourier components in the coupling coefficient of the planar equivalent circuit. To qualitatively illustrate this interpretation, let us consider the structure with wave impedance perturbation corresponding to Figure 3b. We have replaced the shunt capacitances by low impedance transmission line sections of arbitrary length and width and we have numerically calculated the Fourier Transform of the coupling coefficient [23] by means of a *FFT* algorithm using *MATLAB*. The result, shown in Figure 6, points out the rejection of frequency bands related to the presence of capacitances (i.e., due to the low impedance transmission line sections) and characterized by the high power frequency components. Additionally, between those components, lower peaks are indicative of the suppression of undesired spurious passbands. Even though the perturbation function is a sinusoid, the Fourier Transform of the coupling coefficient reveals that multiple frequency bands are rejected, this being in agreement with Figure 3b, and interpreted within the framework of coupled mode

theory. A quantitative analysis based on the equivalent circuit model is not possible since the dimensions of the low impedance transmission line sections are frequency dependent. This justifies the arbitrariness of the transmission line sections emulating the shunt capacitors.

4. SIMULATIONS AND MEASUREMENTS

To validate the analysis of the previous sections, we have simulated two PL-EBG-CPW structures with square wave geometry and lumped capacitances. To this end, the commercial software *ADS-Agilent Technologies* has been used. One of the structures corresponds to case A, i.e., $\lambda_T = 2l$, while in the other one, the period of the perturbation has been chosen according to $\lambda_T = 2l/3$. For the simulations and design of the structures, the parameters of the *Rogers RO3010* substrate have been used ($\varepsilon_r = 10.2$, thickness $h = 1.27$). In the latter case, the results of the simulation are compared with measurements obtained on fabricated structures. To avoid the presence of lumped devices (which degrade the response at high frequencies and complicate the fabrication process), a completely planar PL-EBG-CPW has been also designed and fabricated, with the lumped elements replaced by T-shaped capacitors. Let us now consider these structures separately.

Structure A: $\lambda_T = 2l$ (lumped reactances)

To design the structure, we first set the electrical parameters of the unperturbed PL-CPW, i.e., a Bragg frequency of $f_B = 0.9\,\text{GHz}$ and a Bloch impedance (i.e., impedance seen from the ports) of 50Ω. By using 4.4 pF shunt reactances (2.2 pF *phicom* capacitors disposed in parallel pairs) the wave impedance of the unloaded line is found to be 81Ω. From this, the lateral dimensions of the coplanar waveguide have been obtained: the width of the central strip is $W = 2\,\text{mm}$, while the distance to ground planes is $G = 2.5\,\text{mm}$. To determine the distance between adjacent capacitor pairs, l, we need to know the lower frequency of the first spurious band. If this is set to 2.3 GHz, then $l = 3.4\,\text{cm}$. The *LineCalc* transmission line calculator (included in *ADS-Agilent Technologies*) has been used to determine the dimensions of the structure. Finally, to obtain the layout of the PL-EBG-CPW, 15Ω step variations of wave impedance around the central value have been considered, resulting in a square wave geometry, where G alternates between 1.52 mm and 3.65 mm (the conductor strip width being uniform). Figure 7 shows the simulated transmission coefficient of both the perturbed PL-EBG-CPW and unperturbed PL-CPW structures. Rejection in all bands occurs (including the first passband),

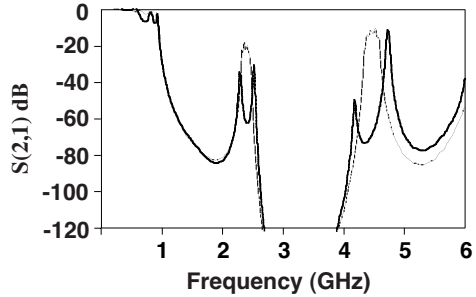

Figure 7. Simulated frequency responses $|S_{21}|$ for the PL-EBG-CPW (bold line) and PL-CPW (thin line) structure considered in case A (stepped geometry). In the vicinity of 3 GHz the responses are affected by the self resonant frequency of the capacitances, giving values below the noise floor, which is ignored in the simulation.

in agreement with the analytical result of Section 2 (equation (4)). Moreover, the magnitude of rejection increases with frequency, also in accordance to that equation. Indeed, for the considered number of sections (6 capacitor pairs), attenuation below the Bragg frequency is not significant although a notch can be appreciated in the vicinity of 0.8 GHz. However, the spurious bands are clearly rejected, with attenuation levels above 50 dB in the central frequency of the bands. It is also worth commenting that no ripple is observed at low frequencies. This is indicative of a perfect match, even for the perturbed structure and is explained by the symmetric variations of wave impedance around the nominal value. The reported simulations and analytical calculation of the previous sections point out that a complete rejection of spurious bands can be achieved by means of a perturbation periodicity covering two capacitor stages ($\lambda_T = 2l$). This suppression of bands can be even more effective and the narrow peaks at both sides of the rejected bands can be attenuated if stronger variations of wave impedance are considered. On the other hand, even though the frequency response is not significantly varied below the cutoff frequency, attenuation in this band might be important if the number of stages is increased. Therefore it is of interest the suppression of undesired bands while leaving the first band unaltered. According to the results of Section 2, this can potentially be achieved if the period of the perturbation is set to $\lambda_T = 2l/3$.

Structure B: $\lambda_T = 2l/3$ *(lumped reactances)*

In this case, not only comparative simulations of the perturbed

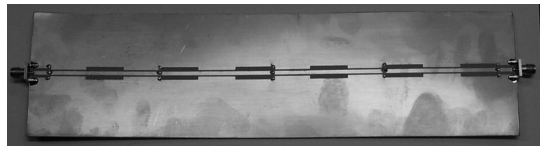

Figure 8. Fabricated PL-EBG-CPW structure with five capacitor pairs.

and unperturbed structures will be shown. We will also obtain the measured frequency responses on fabricated devices. Therefore, it is important to design the structure in such a way that a significant portion of the frequency response lies below the self-resonant frequency of shunt reactances (2.2 pF *phicom capacitors*), which is in the vicinity of 3 GHz. For this reason, the Bragg frequency and the lower frequency of the first spurious band have now been set to 0.7 GHz and 1.2 GHz, respectively. Under these conditions, the passbands of the structure are shifted to lower frequencies and the second spurious band is clearly separated from the resonant frequency of shunt capacitances. With these electrical parameters, the geometry of the PL-CPW (unperturbed structure) is given by $W = 2.2\,\text{mm}$, $G = 1.56\,\text{mm}$ and $l = 6.1\,\text{cm}$, resulting in a 50Ω Bloch impedance and 65Ω impedance for the unloaded line. For the design of the PL-EBG-CPW structure, the wave impedance of the line has been modulated with step variations of 15Ω up and down. By maintaining the width of the signal strip uniform, the distance to ground planes has been found to be $G = 0.77\,\text{mm}$ for the low impedance portions and $G = 2.52\,\text{mm}$ for the high impedance sections (the fabricated structure is shown in Figure 8). Figure 9 shows the simulated (using *ADS-Agilent Technologies*) and measured (using a *hp-8753D* network analyzer) frequency responses for the fabricated PL-EBG-CPW and PL-CPW structures. Undistinguishable results below the Bragg frequency are obtained in both structures (simulation and measurement), in agreement with the predictions of Section 2. Above this frequency, suppression of the first and second spurious band with rejection levels above 30 dBs are clearly observed (center frequency). Since the perturbation geometry is a square wave, and the EBG structure has been designed with a fundamental (rejected) frequency centered in the first band, elimination of the second spurious band is actually a result not expected within the framework of coupled mode theory. Nevertheless, rejection of this band is in agreement with the numerical results of Section 2, based on the calculation of the dispersion relation of the structure, and has been explained by the interaction effects between the EBG structure and the periodicity associated to the presence of capacitors. For higher order spurious bands, the self-

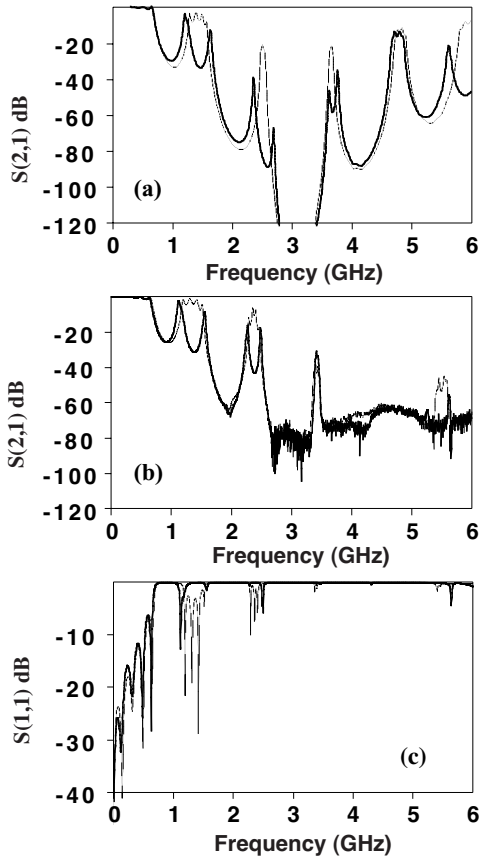

Figure 9. Simulated (a) and measured (b) transmission coefficients $|S_{21}|$ for the fabricated PL-EBG-CPW (bold line) and PL-CPW (thin line) structures. In (c), the measured reflection coefficient $|S_{11}|$ is depicted for both the PL-EBG-CPW (bold line) and PL-CPW (thin line) structures. These results demonstrate the absence of radiation losses.

resonant frequency of shunt capacitors degrades the frequency response and this obscures the effects of the EBG, although these are still visible in the rejection of the fifth band. These results thus demonstrate that a complete rejection of spurious bands can be achieved in periodic loaded coplanar waveguides by means of a very simple perturbation geometry, leaving unaltered the operative bandwidth of the structure (delimited by the Bragg frequency), and the required physical length for the device.

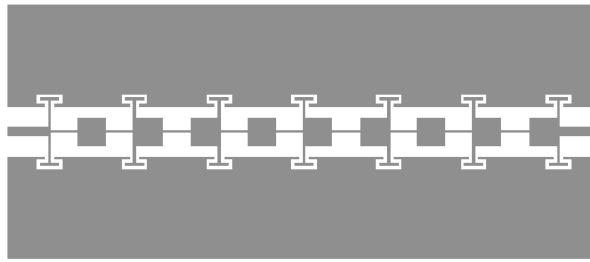

Figure 10. Layout of the planar PL-EBG-CPW structure with seven capacitor stages.

Structure C: $\lambda_T = 2l/3$ (T-shaped capacitances)

Since lumped elements are not present in this case, the structure has been designed to exhibit a cutoff frequency of $f_B = 2.5\,\text{GHz}$, with the result of smaller device dimensions. The distance between adjacent capacitances and the lateral dimensions of the unperturbed structure are $l = 13.3\,\text{mm}$, $W = 1.5\,\text{mm}$ and $G = 3.15\,\text{mm}$. With this geometry, and a nominal value of $C_{ls} = 2.3\,\text{pF}$, the device is matched to a 50Ω impedance, while the characteristic impedance of the unloaded line is $Z_o = 95\Omega$. In order to obtain an efficient rejection of spurious frequencies, the PL-EBG-CPW structure has been designed with 35Ω step variations of wave impedance. To achieve this modulation degree, the strip width has been varied in this case, while the distance between ground planes has not been modified along the device. By means of the LineCalc, it has been found that the strip width oscillates between $W = 0.4\,\text{mm}$ and $W = 4.4\,\text{mm}$ in the high and low impedance sections of the structure. Obviously, the dimensions of the T-shaped capacitors, have been determined to provide the nominal value of capacitance (i.e., $C_{ls}/2$). To this end, full wave em simulations have been carried out by means of the commercial software CST Microwave Studio on reference T-shape based structures. The layout of the fabricated device is shown in Fig. 10. Fig. 11 shows the measured frequency response, compared to that obtained on the unperturbed (uniform strip width) structure. As can be seen, significant attenuation of the spurious frequencies is achieved, while the passband of the structure is not affected by the step variations in strip width. The proposed planar structures exhibit therefore low insertion loss in the passband, a very sharp cutoff and a wide stop band.

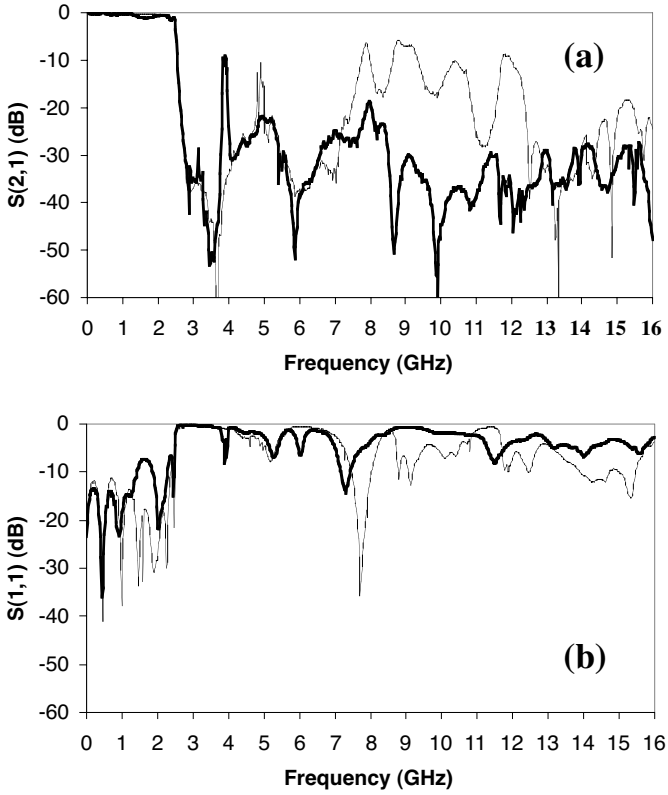

Figure 11. Measured transmission (a) and reflection (b) coefficients for the planar PL-EBG-CPW (bold line) and PL-CPW (thin line) structures.

5. CONCLUSIONS

In this work, the frequency selective behaviour of coplanar waveguides periodically loaded with shunt capacitances, and periodically perturbed by varying the distance between the central strip and ground planes has been studied. With an effort focused on the rejection of the spurious passbands of the device, two EBG structures have been analysed: one of them designed to reject the first spurious band and the other (with longer perturbation period) tuned in the first frequency band (i.e., below the Bragg frequency). To gain insight on the effects of the perturbation geometry, both square wave and sinusoidal functions have been considered. The analysis of these structures, based on the calculation of the dispersion relation, has pointed out that the rejected

spurious bands are not merely given by the Fourier transform of the perturbation geometry. It has been found, for instance, that multiple spurious bands can be suppressed by using a (simply tuned) sinusoid layout pattern. This excess of rejected bands, not explained within the framework of coupled mode theory, has been demonstrated to be due to the presence of capacitors (not accounted for in that theory) and has been interpreted by means of a planar equivalent circuit model of the structure, where the loading capacitors are replaced by low impedance transmission line sections of frequency dependent width and length. On the basis of comparative simulations we have demonstrated the validity of the planar equivalent circuit, where the coupled mode theory is applicable. The key point to qualitatively understand the analytical results is that the geometry of the equivalent circuit is not given by the superposition (addition) of the EBG geometry and the layout associated to the presence of low impedance transmission line sections. We have finally carried out simulations and measurements that support the analysis based on microwave network theory. We have found that all spurious frequency bands are attenuated by using a square wave geometry with perturbation periodicity related to the distance l between adjacent capacitors by $\lambda_T = 2l/3$. In addition, the simulations and measurements indicate that the presence of the EBG does not modify the frequency response below the Bragg frequency. On the basis of a fabricated planar structure with the lumped reactances replaced by T-shaped capacitors and significant wave impedance modulation, it has been experimentally obtained an efficient suppression of spurious bands up to at least 16 GHz. The result is a low pass frequency response with a very wide stop band.

To conclude, it has been demonstrated that multiple frequency bands can be rejected in periodic loaded coplanar waveguides by means of the EBG method, using very simple perturbation geometry. This avoids the need of cascading several EBG stages or superposing various perturbation functions tuned at the desired frequencies [24]. The results of the work open the possibility to fabricate CPW-based microwave and millimetre wave filters, phase shifters and frequency multipliers with improved performance.

ACKNOWLEDGMENT

This work has been supported by DGI and CICYT by project contracts BFM2001-2001 and TIC2002-04528-C02-01, respectively. The authors also thank to DURSI (Generalitat de Catalunya) for supporting this work by means of an ACI action ACI2001-33. Thanks to Dr. Tapani Narhi from ESA for his helpful comments to the paper.

REFERENCES

1. Hsia, R. P., W. M. Zhang. C. W. Domier, and N. C. Luhmann, "A hybrid nonlinear delay line-based broad-band phased antenna array system," *IEEE Microwave and Guided Wave Letters*, Vol. 8, 182–184, 1998.
2. Fernandez, M., E. Delos, X. Melique, S. Arscott, and D. Lippens, "Monolithic coplanar transmission lines loaded by heterostructure barrier varactors for a 60 GHz tripler," *IEEE Microwave and Wireless Components Letters*, Vol. 11, 498–500, Dec. 2001.
3. Barker, N. S. and G. M. Rebeiz, "Distributed MEMS true-time delay phase shifters and wide-band switches," *IEEE Trans. Microwave Theory Tech.*, Vol. 46, 1881–1890, Nov. 1998.
4. Borgioli, A., Y. Liu, A. S. Nagra, and R. A. York, "Low-loss distributed MEMS phase shifter," *IEEE Microwave and Guided Wave Letters*, Vol. 10, 7–9, Jan. 2000.
5. Carman, E., K. Giboney, M. Case, M. Kamegawa, R. Yu, K. Abe, M. J. W. Rodwell, and J. Franklin, "28–39 GHz distributed harmonic generation on a soliton nonlinear transmission line," *IEEE Microwave Guided Wave Lett.*, Vol. 1, 28, 1991.
6. Edwards, T. C. and M. B. Steer, *Foundations of Interconnect and Microstrip Design*, third edition, John Wiley and Sons Ltd, 2000.
7. Yang, F. R., K. P. Ma, Y. Qian, and T. Itoh, "A uniplanar compact photonic-bandgap structure and its applications for microwave circuits," *IEEE Trans. Microwave Theory Tech.*, Vol. 47, 1509, 1999.
8. Joannopoulos, J. D., R. D. Meade, and J. N. Winn, *Photonic Crystals: Molding the Flow of Light*, Princeton University Press, Princeton, NJ, 1995.
9. Peral, E., J. Capmany, and J. Martí, "Iterative solution to the Gel' Fand-Levitan-Marchenko coupled equations and application to synthesis of fiber gratings," *IEEE Journal of Quantum Electronics*, Vol. 32, No. 12, 2078–2084, Dec. 1996.
10. Katsenelenbaum, B. Z., L. Mercader, M Pereyaslavets, M. Sorolla, and M. Thumm, *Theory of Nonuniform Waveguides*, Vol. 44, ser. IEE Electromagn. Waves, London, U.K. IEE Press, 1998.
11. Qian, Y., V. Radistic, and T. Itoh, "Simulation and experiment of photonic band-gap structures for microstrip circuits," *Proc. Asia-Pacific Microwave Conf.*, 585–588, Hong Kong, Dec. 1997.
12. Radistic, V., Y. Qian, R. Coccioli, and T. Itoh, "Novel 2-D photonic band gap structures for microstrip lines," *IEEE Microwave Guided Wave Lett.*, Vol. 8, 69–71, Feb. 1998.

13. Kim, T. and C. Seo, "A novel Photonic bandgap structure for low-pass filter of wide stopband," *IEEE Microwave Guided Wave Lett.*, Vol. 10, 13–15, Jan. 2000.
14. Akalin, T., M. A. G. Laso, T. Lopetegi, O. Vanbesien, M. Sorolla, and D. Lippens, "EBG-type microstrip filtres with one and two-sided patterns," *Microwave and Optical Technology Lett.*, Vol. 30, 69–72, July 2001.
15. Lopetegi, T., M. A. G. Laso, M. J. Erro, D. Benito, M. J. Garde, F. Falcone, and M. Sorolla, "Novel photonic bandgap microstrip structures using network topology," *Microwave Opt. Tech. Lett.*, Vol. 25, 33–36, April 2000.
16. Lopetegi, T., M. A. G. Laso, J. Hernández, M. Bacaicoa, D. Benito, M. J. Garde, M. Sorolla, and M. Guglielmi, "New microstrip wiggly-line filters with spurious passband suppression," *IEEE Trans Microwave Theo Tech.*, Vol. 49, 1593–1598, Sep. 2001.
17. Radisic, V., Y. Qian, and T. Itoh, "Broad-band power amplifier using dielectric photonic bandgap structures," *IEEE Microwave Guided Wave Lett.*, Vol. 8, 13–15, Jan. 1998.
18. Lee, Y-T., J-S. Lim, J-S. Park, D. Ahn, and S. Nam, "A novel phase noise reduction technique in oscillators using defected ground structure," *IEEE Microwave Wireless Comp. Lett.*, Vol. 12, 39–41, Feb. 2002.
19. Yun, T-Y. and K. Chang, "Uniplanar one-dimensional photonic bandgap structures and resonators," *IEEE Trans. Microwave Theory Tech.*, Vol. 49, 549–553, March 2001.
20. Fu, Y-Q., G. H. Zhang, and N. C. Yuan, "A novel EBG coplanar waveguide," *IEEE Microwave and Wireless Components Lett.*, Vol. 11, 447–449, Nov. 2001.
21. Sor, J., Y. Qian, and T. Itoh, "Miniature low loss CPW periodic structure for filter applications," *IEEE Trans. Microwave Theory Tech.*, Vol. 49, 2336–2341, December 2001.
22. Pozar, D. M., *Microwave Engineering*, Addison Wesley, Reading, MA, 1990.
23. Lopetegi, T., M. A. G. Laso, M. J. Erro, M. Sorolla, and M. Thumm, "Analysis and design of EBG structures for microstrip lines by using the coupled mode theory," *IEEE Microwave and Wireless Components Lett.*, Vol. 12, 441–443, November 2002.
24. Laso, M. A. G., T. Lopetegi, M. J. Erro, D. Benito, M. J. Garde, and M. Sorolla, "Multiple-frequency tuned photonic bandgap microstrip structures," *IEEE Microwave and Guided Wave Lett.*, Vol. 10, 220–222, June 2000.